Microbubble Persistence in the Microcirculation During Ischemia/Reperfusion and Inflammation Is Caused by Integrin- and Complement-Mediated Adherence to Activated Leukocytes

Jonathan R. Lindner, MD; Matthew P. Coggins, BA; Sanjiv Kaul, MD; Alexander L. Klibanov, PhD; Gary H. Brandenburger, PhD; Klaus Ley, MD

Background—Albumin microbubbles that are used for contrast echocardiography persist within the myocardial microcirculation after ischemia/reperfusion (I-R). The mechanism responsible for this phenomenon is unknown.

Methods and Results—Intravital microscopy of the microcirculation of exteriorized cremaster muscle was performed in 12 wild-type mice during intravenous injections of fluorescein-labeled microbubbles composed of albumin, anionic lipids, or cationic lipids. Injections were performed at baseline and after 30 to 90 minutes of I-R in 8 mice and 2 hours after intrascrotal tumor necrosis factor-α (TNF-α) in 4 mice. Microbubble adherence at baseline was uncommon ($<$2/50 high-power fields). After I-R, adherence increased ($P<0.05$) to 9 ± 5 and 5 ± 4 per 50 high-power fields for albumin and anionic lipid microbubbles, respectively, due to their attachment to leukocytes adherent to the venular endothelium. TNF-α produced even greater microbubble binding, regardless of the microbubble shell composition. The degree of microbubble attachment correlated ($r=0.84$ to 0.91) with the number of adhered leukocytes. Flow cytometry revealed that microbubbles preferentially attached to activated leukocytes. Albumin microbubble attachment was inhibited by blocking the leukocyte β_2-integrin Mac-1, whereas lipid microbubble binding was inhibited when incubations were performed in complement-depleted or heat-inactivated serum rather than control serum.

Conclusions—Microvascular attachment of albumin and lipid microbubbles in the setting of I-R and TNF-α–induced inflammation is due to their β_2-integrin– and complement-mediated binding to activated leukocytes adherent to the venular wall. Thus, microbubble persistence on contrast ultrasonography may be useful for the detection and monitoring of leukocyte adhesion in inflammatory diseases. **(*Circulation*. 2000;101:668-675.)**

Key Words: microcirculation ■ echocardiography ■ leukocytes ■ ischemia ■ reperfusion

Although the microvascular rheology of sonicated albumin microbubbles is similar to that of red blood cells (RBCs) in normal myocardium,[1,2] their microcirculatory transit is abnormally prolonged in myocardial regions undergoing ischemia followed by reperfusion (I-R).[3] The exact mechanism for the persistence of albumin microbubbles in injured tissue is not known. Based on experimental observations, proposed putative mechanisms include charge-specific interactions with the endothelium in regions where the glycocalyx is compromised[3] and direct adherence to exposed subendothelial extracellular matrix.[4]

Many different processes contribute to the structural and functional abnormalities of the microcirculation after I-R. Oxygen-derived free radicals play a role in early inflammatory responses after reperfusion and promote leukocyte adhesion.[5] This response is characterized by local chemokine release, expression of leukocyte adhesion molecules on the endothelial surface, and activation of leukocyte integrins.[6,7] Integrins, which are responsible for the firm adhesion of leukocytes on the endothelium of postcapillary venules, also mediate leukocyte interactions with denatured proteins,[8,9] including albumin, which forms the shell of several microbubble contrast agents.[10] Serum complement proteins are also important in the immune response after I-R.[11] Among other functions, complement proteins promote the phagocytosis of foreign or abnormal particles by attaching to their surface and then binding to complement receptors on leukocytes. This process of opsonization is at least in part responsible for interactions between leukocytes and liposomal membranes,[12,13] the shells of which are similar to those of lipid microbubble agents.[10]

In the present study, we hypothesized that activated leukocytes adherent to the venular endothelial surface bind micro-

Received May 24, 1999; revision received August 5, 1999; accepted August 13, 1999.

From the Cardiovascular Division (J.R.L., M.P.C., S.K.) and the Department of Biomedical Engineering (S.K., K.L.), University of Virginia School of Medicine, Charlottesville, Va; and Mallinckrodt Medical, Inc (A.L.K., G.H.B.), St Louis, Mo.

Correspondence to Jonathan R. Lindner, MD, Box 158, Cardiovascular Division, University of Virginia Medical Center, Charlottesville, VA 22908. E-mail jlindner@virginia.edu

Circulation **is available at http://www.circulationaha.org**

bubbles and contribute to their prolonged transit after I-R. Intravital microscopy was used to investigate the interactions between microbubbles and activated leukocytes in vivo. The hypothesis that leukocyte integrins, serum complement, or both are responsible for these interactions was tested in vitro with the use of flow cytometry.

Methods

Materials and Antibodies

Fluorescein-labeled perfluorocarbon-filled microbubbles with shells composed of albumin (Optison; Mallinckrodt Medical, Inc) or lipids containing either anionic or cationic components ($MP1950^-$ and $MP1950^+$, respectively; Mallinckrodt Medical, Inc) were used. The mean sizes for these microbubbles ranged from 3.9 to 5.4 μm, and their mean concentrations, measured before each experiment with the use of an hemocytometer (Fisher Scientific), ranged from 1.8 to 4.0×10^8/mL.

Murine anti-human monoclonal antibodies (MAbs) were used for the in vitro experiments to block leukocyte integrins Mac-1 ($\alpha_m\beta_2$) and VLA-4 ($\alpha_4\beta_1$); these included 2LPM19c (DAKO), an IgG_1 against the human CD11b (α_m) component of Mac-1, and P4G9 (DAKO), an IgG_3 against the human CD49d (α_4) component of VLA-4. Murine IgG_1 antibody (Biodesign International) with no known cross-reactivity with human cells was used as a nonbinding control, and BL-E/G3 (Biodesign International), a murine IgG_1 against human CD43, was used as a leukocyte-binding control MAb. Flow cytometry performed after indirect immunostaining with FITC-conjugated goat anti-mouse IgG $F(ab')_2$ (Biodesign International) confirmed that 2LPM19c bound mostly to neutrophils and monocytes, that P4G9 bound mostly to lymphocytes, and that BL-E/G3 bound to all leukocytes.

Control serum was obtained from healthy adult volunteers, and a portion was placed in a 57°C water bath for 30 minutes to inactivate the complement. Complement-depleted human serum (Quidell Corp) treated with methylamine and containing 2 mmol/L $CaCl_2$ and $MgCl_2$ was used to evaluate the importance of the C3 component in microbubble attachment.

Animal Preparation

The study protocol was approved by the Animal Research Committee at the University of Virginia. Twelve male wild-type C57BL/6 mice weighing between 22 and 31 g were anesthetized with an intraperitoneal injection (12.5 μL/g) of a solution containing 10 mg/mL ketamine hydrochloride, 1 mg/mL xylazine, and 0.02 mg/mL atropine. Body temperature was maintained at 37°C with a heating pad. Both jugular veins were cannulated for the administration of microbubbles and drugs. Anesthesia was maintained with the intravenous administration of 0.1 mg pentobarbital every ≈45 minutes as needed.

Either the right or the left cremaster muscle was prepared for intravital microscopy as previously described.[14] The muscle was exteriorized through a scrotal incision and secured to a translucent pedestal. A longitudinal incision was made in the muscle, the edges were secured to the pedestal, and the epididymis and testicle were gently pinned to the side. The preparation was superfused continuously with isothermic bicarbonate-buffered saline.

Intravital Microscopy

Microscopic observations were made with an intravital microscope (Axioskop FS; Carl Zeiss, Inc) with a saline immersion objective (SW 40/0.75 numerical aperture). Epifluorescence was performed with an excitation filter for fluorescein (450 to 490 nm) with a light source interfaced to a strobe (model 11360; Chadwick-Helmuth) that flashed at 30 Hz. Video recordings were made with a high-resolution camera (VE-1000CD; Dage-MTI) connected to an S-VHS recorder (Panasonic; Matsushita Electric Co). Centerline venular RBC velocities were measured with a dual photodiode[15] and converted to mean blood flow velocities through multiplication by an empirical factor of 0.625.[16] Shear rates (γ_w) were determined with the following equation:

$$\gamma_W = 2.12(8V_b)/d$$

where V_b is the mean blood velocity, d is the vessel diameter, and 2.12 is a correction factor for the shape of the velocity profile.[17]

Venular diameters were measured off-line with the use of video calipers. Freeze-frame advancing allowed the tracking of individual rolling leukocytes over a distance of 30 to 100 μm. The total distance traveled was divided by the elapsed time to derive the mean rolling velocity. The number of rolling leukocytes was determined by counting leukocytes crossing a line perpendicular to the vessel for 1 minute. Leukocyte rolling flux fraction (F), which reflects the percentage of leukocytes passing through a venule that are rolling, was calculated with the following equation:

$$F = r_n/(0.25\pi d^2 \cdot V_b \cdot 60 \cdot C_L)$$

where r_n is the number of rolling leukocytes in 1 minute, d is the vessel diameter, V_b is the centerline blood velocity, and C_L is the systemic blood leukocyte concentration.[18] Adherent leukocytes, which are defined as those not moving for ≥30 seconds, were counted and expressed per venular surface area, calculated from the diameter and length measured with the use of video calipers (with the assumption of cylindrical geometry).

In Vivo Protocols

Eight wild-type mice were used to assess microbubble behavior after I-R. Before ischemia, 3 cremaster venules with diameters of 25 to 40 μm were recorded under transillumination for 1 minute each, followed by the measurement of centerline blood velocity. Approximately 4.0×10^7 microbubbles of each type (volume range 100 to 220 μL) were injected in random order separated by periods of 8 to 10 minutes. At 2 minutes after each injection, 50 random high-power fields, encompassing arterioles, venules, and capillaries, were scanned for ≈2 minutes with the use of fluorescent epi-illumination. Brief transillumination was used to confirm the presence of normal flow in a vessel when adherent microbubbles were identified. Blood flow was then interrupted for 30 to 90 minutes with the use of a ligature placed around the cremasteric artery just proximal to the muscle and, if present, around the major feeding artery connecting the cremaster to the epididymis. The microcirculation was monitored to ensure cessation of flow over the entire ischemic period. After 20 minutes of reflow, microbubble administration was again performed as described. The 3 venular segments recorded before ischemia were identified, and postreperfusion video recordings and velocity measurements were made.

Four wild-type mice were studied to assess microbubble behavior during tumor necrosis factor-α (TNF-α)–induced inflammation. Intrascrotal injections of 0.5 μg murine recombinant TNF-α (Genzyme Corp) in 0.2 mL saline were performed 2 hours before dissection of the cremaster muscle. Video recordings and velocity measurements of 3 venules and microbubble injections were performed in a manner similar to the I-R protocol.

Flow Cytometry

Blood was obtained from healthy adult volunteers and anticoagulated with heparin (10 U/mL). The cellular fraction was separated through centrifugation and washed twice. Leukocytes were labeled with 1 μmol/L rhodamine-6G (Molecular Probes) for 30 minutes. Cells were then washed, resuspended in PBS, and analyzed for leukocyte concentration through the use of hemocytometric measurements of Kimura-stained samples. A portion of the cells were activated by 10 nmol/L phorbol-12-myristate-13-acetate (PMA) (Sigma Chemical Co) for 15 minutes at 37°C before use.

Approximately 2×10^6 activated or nonactivated leukocytes were placed in 0.2 mL of PBS containing 2 mmol/L $MgCl_2$ and combined with 2×10^7 albumin or $MP1950^-$ microbubbles. Total volume was brought to 0.5 mL by the addition of serum, heat-inactivated serum, or C3-depleted serum. Additional samples containing serum were

Venular Hemodynamic Parameters and Leukocyte Rolling and Adhesion Data

	I-R		
	Baseline	Reperfusion	TNF-α
Venules, n	24	18	12
Venular diameter, μm	34.6±6.4	35.8±6.2	36.8±4.6
Blood velocity, μm/s	1152±321	1449±311*	1021±388
Wall shear rate, s^{-1}	962±234	1198±427*	775±344
Leukocyte flux fraction	0.19±0.06	0.14±0.09	0.11±0.10
Leukocyte rolling velocity, $\mu m/s^{-1}$	36.7±19.3	28.8±18.0†	12.2±14.5‡
Leukocyte adherence, mm^{-2}	365±117	603±136†	1206±81‡

*$P<0.05$ compared with TNF-α data.
†$P<0.05$ compared with baseline data.
‡$P<0.01$ compared with both baseline and reperfusion data.

prepared that contained 10 μg of binding or nonbinding control antibody, 2LPM19c, or P4G9. All samples were gently agitated during 3-minute incubations at 37°C. RBCs present in the samples were hypotonically lysed with NH_4Cl (150 mmol/L). Suspensions were analyzed with a flow cytometer (FACScan; Becton Dickinson), and the results of 3 separate studies were averaged. Differences between leukocyte and microbubble side and forward light scatter permitted the exclusion (through gating) of free microbubbles from analysis. Data are displayed as green (fluorescein)-versus-red (rhodamine) fluorescence and as histograms of green fluorescence in a gated population.

Statistical Analysis

Data are expressed as mean±SD. Comparisons of behavior of different microbubbles were made with repeated measures ANOVA. Correlations between leukocyte rolling or adherence and microbubble attachment were made with multiple regression analysis. Differences were considered significant at $P<0.05$ (2-sided).

Results

Hemodynamics and Leukocyte Adhesion After I-R and TNF-α

Ischemia was followed by successful reperfusion of the cremaster muscle in 6 of 8 mice. The duration of ischemia was 30, 60, or 90 minutes (2 mice each). In mice undergoing I-R, venular mean blood flow velocity and shear rate were slightly higher after reperfusion compared with baseline, probably as a result of hyperemia (Table 1). Leukocyte rolling was observed in postcapillary venules even before ischemia (Table 1). The mean rolling velocity (36.9± 19.3 μm/s) and flux fraction (0.19±0.06) were consistent with those previously reported early after exteriorization of the cremaster muscle.[14] Under these conditions, rolling is mediated by rapid mobilization of P-selectin on the endothelial surface after surgical trauma.[14] After I-R, the mean leukocyte flux fraction decreased slightly, and the mean rolling velocity decreased significantly by 22%. The mean number of adherent leukocytes nearly doubled after I-R. There was no relation between the duration of ischemia and either rolling flux fraction or the number of adherent leukocytes.

Compared with I-R, TNF-α resulted in a more pronounced reduction in mean leukocyte rolling velocity and greater adherence (Table 1). The low calculated leukocyte flux fraction is characteristic of TNF-α–induced inflammation[19] and most likely results from the rapid arrest of leukocytes after rolling for a limited distance.[20]

Microbubble Behavior After I-R and TNF-α

At baseline, almost all microbubbles passed unimpeded through the microcirculation, whereas after I-R and TNF-α activation, many attached to the surface of leukocytes adherent to the endothelial surface of postcapillary venules. Figure 1 illustrates venules from 2 different mice after I-R (Figure 1A) and TNF-α activation (Figure 1B). Images obtained through transillumination demonstrated a greater degree of leukocyte adherence after TNF-α. Fluorescent epi-illumination of the same venular segments revealed the attachment of fluorescein-labeled albumin microbubbles to individual leukocytes (Figure 1A) or to clusters of leukocytes (Figure 1B) adherent to the venular surface. Occasionally, adherent leukocytes coupled with microbubbles were seen to detach and either roll for a short distance and adhere in a new location or to join streamline flow, conveying the microbubbles with them.

The mean numbers of microbubbles that attached to adherent leukocytes are depicted in Figure 2. At baseline, microbubble attachment was uncommon (<2 per 50 high-power fields) and increased after I-R for the albumin and $MP1950^-$ but not the $MP1950^+$ microbubbles. In comparison, TNF-α resulted in much greater attachment for all 3 microbubble agents. Microbubble rolling along the endothelial surface was uncommon (6% of all interacting microbubbles) and was due to attachment to slowly (<10 μm/s) rolling leukocytes. Significant correlations ($r=0.84$ to 0.91) were noted between the attachment of microbubbles and the degree of leukocyte adhesion (Figure 3). There was no correlation between microbubble attachment and leukocyte rolling flux fraction.

Flow Cytometry

Potential mechanisms of interactions between leukocytes and microbubbles were evaluated with the use of flow cytometry. Leukocytes were gated according to their characteristic forward and side scatter (Figure 4A), which excluded events attributable to free microbubbles. Activated leukocytes labeled with rhodamine-6G had high red fluorescent activity with little overlap into the green spectrum (Figure 4B).

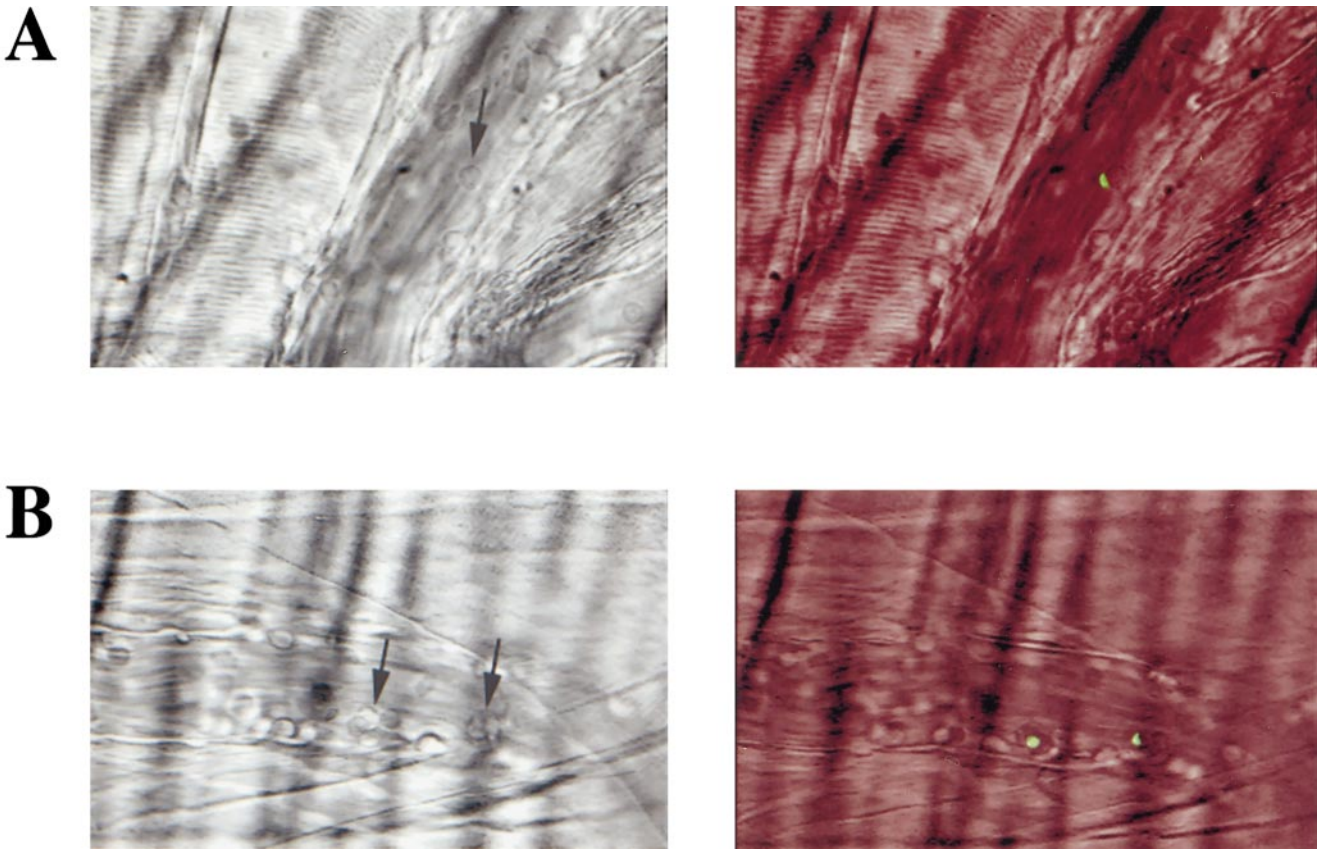

Figure 1. Images obtained during transillumination (left) and fluorescent epi-illumination (right) of venular segments after I-R (A) and TNF-α (B) after intravenous injections of fluorescein-labeled albumin microbubbles. A, 25% of leukocytes visible in venule were adherent, and remainder were rolling. B, 70% of leukocytes were adherent, and remainder were rolling. Arrows denote leukocytes adherent to the venule to which microbubbles attached. See text for details.

Interactions between leukocytes and fluorescein-labeled microbubbles were indicated by the appearance of events in the upper right quadrant (combined red and green fluorescence) when cells were combined with albumin or MP1950$^-$ microbubbles (Figure 4B). Wide variability in the extent of green fluorescence likely represented variation in microbubble size and the number of microbubbles attached to each leukocyte. The percentage of leukocytes binding albumin or MP1950$^-$ microbubbles was 51±8% and 46±8%, respectively.

In the green fluorescence histograms, activated leukocytes exhibited little activity, whereas albumin microbubbles were strongly fluorescent (Figure 5). When incubated together, leukocyte/microbubble complexes were evident on the basis of the appearance of green fluorescence associated with leukocytes and occurred to a much greater extent with activated than with nonactivated leukocytes (311±34% increase in proportion of cells binding fluorescent microbubbles). Free microbubbles were excluded from these analyses by their scatter characteristics. A slight rightward shift of leukocytes without microbubbles was observed reflecting the nonspecific absorption of free fluorochrome, and greater fluorescence for complexes compared with microbubbles alone likely represents the attachment of multiple microbubbles. Interactions between albumin microbubbles and activated leukocytes were largely blocked (61±8% reduction in proportion of cells binding microbubbles) by the MAb against the CD11b component of Mac-1 (2LPM19c). No inhibition occurred with the MAb against VLA-4 (P4G9), the isotype control, or the binding control MAb against CD43. There was a small inhibitory effect when activated leukocytes and albumin microbubbles were incubated in the presence of heat-inactivated or C3-depleted rather than control serum.

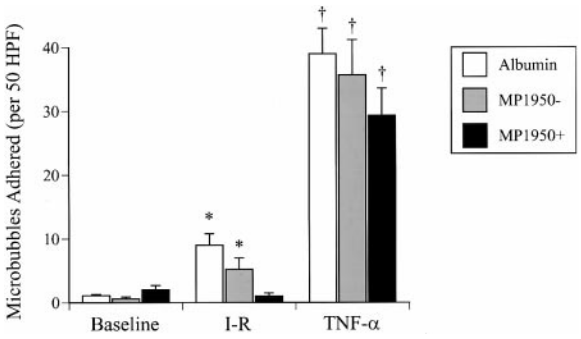

Figure 2. Mean±SEM number of microbubbles persisting within microcirculation at baseline, after I-R, and after TNF-α. HPF indicates high-power field. *$P<0.05$ compared with baseline. †$P<0.01$ compared with baseline and I-R.

As illustrated by the examples in Figure 6, the extent of MP1950$^-$ microbubble attachment was greater with activated than with nonactivated leukocytes (232±34% increase in proportion of cells binding microbubbles). Attachment was not inhibited by MAb against Mac-1, VLA-4, or either of the

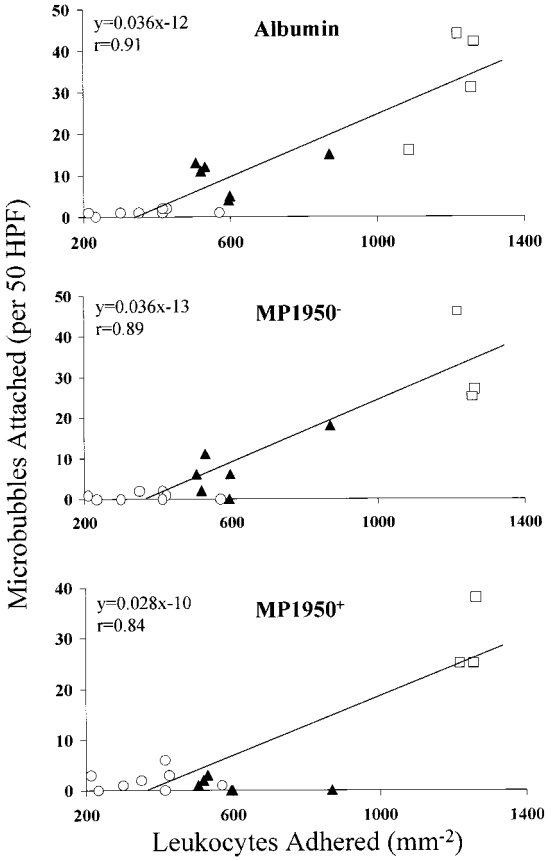

Figure 3. Relation between mean number of adherent leukocytes and number of adhered microbubbles in 50 high-power fields (HPFs) in mice at baseline (○), after I-R (▲), and with TNF-α (□).

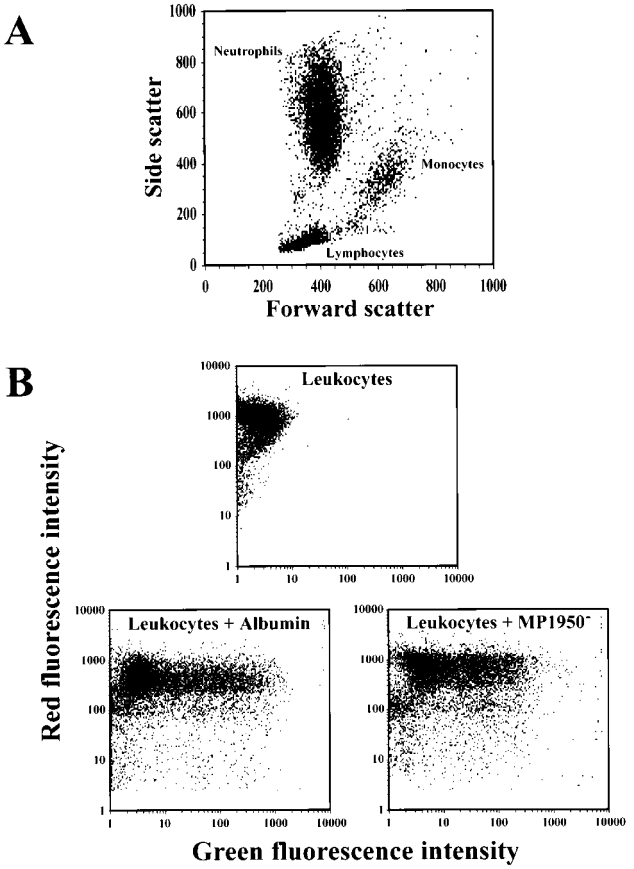

Figure 4. Flow cytometry data illustrating side vs forward light scatter gated to leukocyte population (A) and green vs red fluorescent intensity for rhodamine-6G–labeled leukocytes alone and in combination with binding fluorescein-labeled albumin or MP1950⁻ microbubbles (B).

control antibodies. MP1950⁻ attachment was greatly diminished when incubations were performed in heat-inactivated or C3-depleted serum (73±10% and 71±12% reduction in proportion of cells binding microbubbles).

Discussion

The new finding of this study is that albumin and lipid microbubbles bind to activated leukocytes that have adhered to postcapillary venules in response to I-R or cytokine-induced inflammation. Interactions between leukocytes and albumin microbubbles are mediated largely by leukocyte β_2-integrins, whereas those between leukocytes and lipid microbubbles are mediated by serum complement. Together, these findings suggest that microbubble agents traditionally used to assess perfusion may also have applications for the noninvasive assessment of inflammation.

Affinity of Microbubbles for Inflamed Microvessels

One aim of the present study was to define the mechanisms responsible for the persistent myocardial opacification after albumin microbubble injections into injured vascular beds.[3,21] Previous studies have described normal appearance (wash-in) rates but delayed decay (wash-out) rates of albumin microbubbles after I-R.[3] These results are consistent with the microbubble/leukocyte interactions observed in the present study. We previously postulated that the disruption of the negatively charged glycocalyx, resulting from oxygen-derived free radical formation after I-R,[22] could promote attachment of anionic albumin microbubbles to the endothelial surface.[3] More severe endothelial injury may also expose the subendothelial matrix to which albumin microbubbles may adhere.[4] Although we did not directly study the glycocalyx or endothelial cell integrity in the present study, our results indicate that activated leukocytes play an even more important role in microbubble attachment after I-R. The previous association between microbubble persistence and glycocalyx injury may be indirect, because disruption of the glycocalyx may promote the adhesion of leukocytes.[23]

Our hypothesis that microbubbles adhere preferentially to activated leukocytes via certain adhesion molecules was based in part on our observations that microbubbles attached only to adherent or very slowly rolling leukocytes. Trauma incurred during exteriorization of the cremaster muscle results in leukocyte rolling in venules, mediated by interactions between endothelial P-selectin and its glycoprotein ligand on the leukocyte surface.[14,18] This early leukocyte rolling neither requires nor causes leukocyte activation but rather represents an initial step of the inflammatory cascade.[24] Microbubble attachment to rolling leukocytes at baseline was not observed.

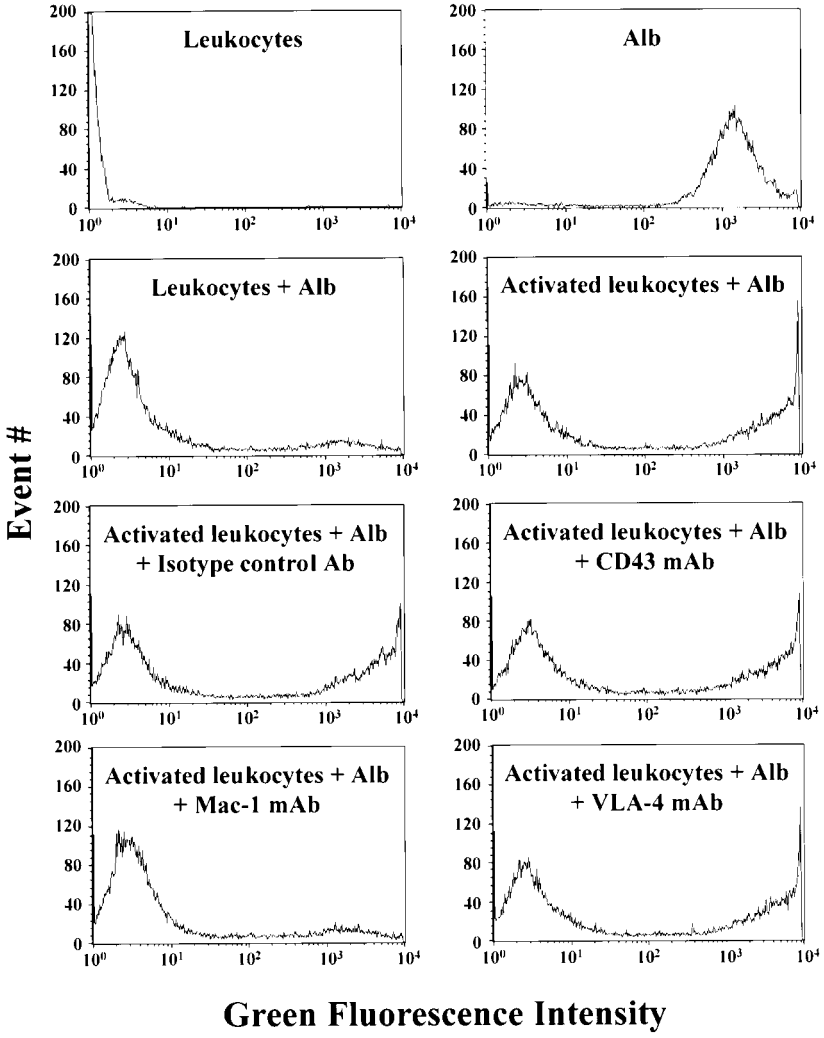

Figure 5. Histograms of green fluorescent intensity from flow cytometry of leukocytes and albumin microbubbles (Alb) alone and in combination. Events were gated to exclude free microbubbles except for panel illustrating microbubbles alone. Microbubble attachment to activated leukocytes was inhibited by 61% by MAb against Mac-1. See text for details.

The arrest of leukocytes is mediated in large part by integrins that, when activated, interact with immunoglobulin receptors (ICAM-1, VCAM-1) and other ligands on the endothelial surface.[24] In this study, firm leukocyte adherence at baseline caused by surgical trauma was very limited and appeared to be responsible for the few microbubbles persisting before ischemia. Venular leukocyte adhesion was much more pronounced after I-R or TNF-α activation. The extent of microbubble attachment in the microcirculation correlated with the number of adherent leukocytes. The few instances in which microbubbles attached to rolling leukocytes occurred mostly in mice treated with TNF-α. The rolling velocities of these leukocyte were very slow, which likely represents β_2-integrin activation.[20] In accordance with these findings, microbubble attachment to leukocytes measured with flow cytometry was markedly enhanced when leukocytes were activated with PMA.

Mediators of Microbubble/Leukocyte Interactions

The finding that albumin microbubble binding to leukocytes is mediated by the β_2-integrin Mac-1 is not unexpected. Mac-1 plays a critical role in neutrophil and monocyte adhesion to various substrates, including many proteins normally found in the extracellular matrix and serum, such as albumin.[8,9,25] The binding of isolated human leukocytes and monocyte-differentiated HL-60 cells to albumin after their activation with PMA or formyl-methionyl-leucyl-phenylalanine can be almost entirely inhibited by MAb blockade of the CD18 subunit of the β_2-integrins[8,9] or the CD11b subunit specific for Mac-1.[7] In the present study, in vitro interactions between activated leukocytes and albumin microbubbles were greatly inhibited by an MAb against Mac-1 that has been shown to inhibit neutrophil binding to ICAM-1 and fibrinogen by blocking the I domain on the CD11b subunit.[26,27] Neither VLA-4, which has been reported to bind denatured albumin,[28] nor complement was necessary for binding.

Our finding that lipid microbubbles persist in the microcirculation during injury by means of attachment to activated leukocytes is new. Earlier investigations have identified mechanisms responsible for leukocyte interactions with liposomes, which are similar in shell composition to lipid microbubbles. Both leukocytes and phagocytic cells of the reticuloendothelial system bind liposomes in a process that is at least in part complement dependent and influenced by the membrane lipid composition.[12,13,29] Complement-mediated uptake is greater for charged than for neutral liposomes.[13,29] Our results indicate that anionic lipid microbubbles similarly

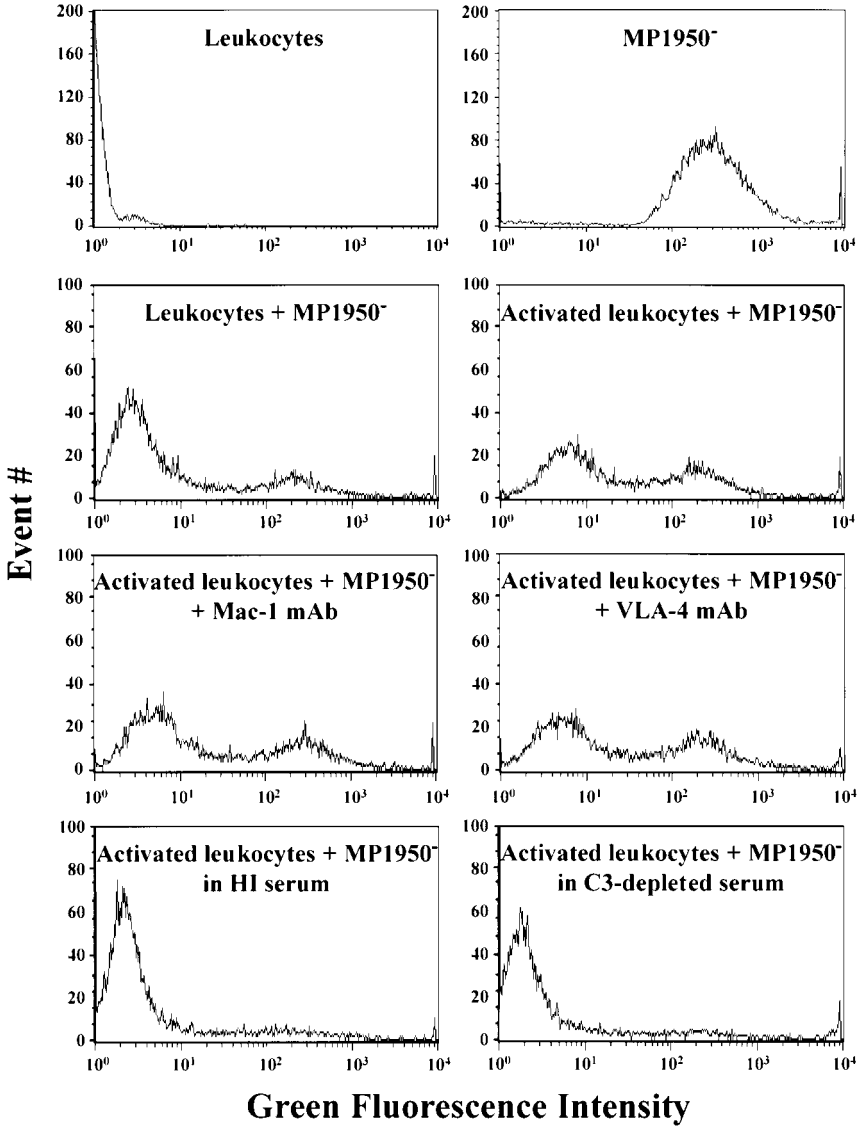

Figure 6. Histograms of green fluorescent intensity from flow cytometry of leukocytes and MP1950⁻ microbubbles alone and in combination. Events were gated to exclude free microbubbles except for panel illustrating microbubbles alone. Microbubble attachment to activated leukocytes when incubations were performed with heat-inactivated (HI) or C3-depleted serum compared with control serum were inhibited by 81% and 78%, respectively. See text for details.

attach to activated leukocytes in a complement-dependent fashion. The enhanced binding of lipid microbubbles when leukocytes were activated with PMA is consistent with known inducible surface expression of complement receptors.[30]

Study Limitations

In the present study, microbubble behavior was assessed in the cremaster muscle rather than the myocardium where initial observations of microbubble persistence were made. Although intravital microscopy of cardiac tissue is possible,[31] the resolution is limited and rapid scanning of multiple fields is difficult. Whether microbubbles attach to circulating leukocytes could not be determined with the use of intravital microscopy.

Although both anionic and cationic lipid microbubbles attached to leukocytes after TNF-α activation, only the anionic microbubbles appeared to bind after I-R. Complement-dependent clearance of liposomes varies according to charge, with anionic and cationic liposomes preferentially activating the classic and alternate pathways, respectively.[13] I-R preferentially activates complement via the classic pathway,[11] which is consistent with the observation of preferential binding of anionic microbubbles in this setting.

Although leukocyte interactions with albumin microbubbles were greatly attenuated with 2LPM19c, they were not eliminated. The mechanisms responsible for residual binding were not elucidated in the study, although some of the most likely mediators were ruled out. Potential mechanisms for complement-independent interactions between lipid microbubbles and leukocytes remain to be explored and include direct adsorption or leukocyte scavenger receptors.[32]

Clinical Implications

The interactions between activated leukocytes and microbubbles described in the present study suggest that the degree of contrast enhancement may provide a means to diagnose and quantify inflammation in almost any organ system that is accessible to ultrasound imaging. This application would have clinical potential in the management of a wide range of disorders without recourse to more invasive procedures, such

as tissue biopsy, or less specific serologic markers of inflammation. Microbubble/leukocyte interactions could be also used to localize drug- or gene-conjugated microbubbles to specific sites of inflammation and then to destroy them with ultrasonography,[33] thereby providing high local concentrations of these agents. Further studies are required to define the clinical potential of our observations.

Acknowledgments

This work was supported in part by grants K08-HL-03810 (to Dr Lindner), R01-HL48890 (to Dr Kaul), and R01-HL64381 (to Dr Ley) from the National Institutes of Health. Matthew P. Coggins is the recipient of a student research grant from the American Diabetes Association, Phoenix, Ariz. The authors are grateful to Eric Kunkel, PhD, and Kai Singbartl, MD, for their valuable discussions.

References

1. Keller MW, Segal SS, Kaul S, Duling B. The behavior of sonicated albumin microbubbles within the microcirculation: a basis for their use during myocardial contrast echocardiography. *Circ Res*. 1989;65: 458–467.
2. Jayaweera AR, Edwards N, Glasheen WP, Villanueva FS, Abbott RD, Kaul S. In vivo kinetics of air-filled albumin microbubbles during myocardial contrast echocardiography: comparison with radiolabeled red blood cells. *Circ Res*. 1994;74:1157–1165.
3. Lindner JR, Ismail S, Spotnitz WD, Skyba DM, Jayaweera AR, Kaul S. Albumin microbubble persistence during myocardial contrast echocardiography is associated with microvascular endothelial glycocalyx damage. *Circulation*. 1998;98:2187–2194.
4. Villanueva FS, Jankowski RJ, Manaugh C, Wagner WR. Albumin microbubble adherence to human coronary endothelium: implications for assessment of endothelial function using myocardial contrast echocardiography. *J Am Coll Cardiol*. 1997;30:689–693.
5. Granger DN, Benoit JN, Suzuki M, Grisham MB. Leukocyte adherence to venular endothelium during ischemia-reperfusion. *Am J Physiol*. 1989; 257:G683–G688.
6. Kurose I, Anderson DC, Miyasaka M, Tamatani T, Paulson JC, Todd RF, Rusche JR, Granger DN. Molecular determinants of reperfusion-induced leukocyte adhesion and vascular protein leakage. *Circ Res*. 1994;74: 336–343.
7. Ichikawa H, Flores S, Kvietys PR, Wolf RE, Yoshikawa T, Granger DN, Aw TY. Molecular mechanisms of anoxia/reoxygenation-induced neutrophil adherence to cultured endothelial cells. *Circulation*. 1997;81: 922–931.
8. Davis GE. The Mac-1 and p159,95 β_2 integrins bind denatured proteins to mediate leukocyte cell-substrate adhesion. *Exp Cell Res*. 1992;200: 242–252.
9. Ley K, Lundgren E, Berger E, Arfors KE. Shear-dependent inhibition of granulocyte adhesion to cultured endothelium by dextran sulfate. *Blood*. 1989;73:1324–1330.
10. Kaul S. Myocardial contrast echocardiography. *Curr Probl Cardiol*. 1997;22:551–635.
11. Collard CD, Vakeva A, Bukusoglu C, Zund G, Sperati CJ, Colgan SP, Stahl GL. Reoxygenation of hypoxic human umbilical vein endothelial cells activates the classic complement pathway. *Circulation*. 1997;96: 326–333.
12. Wassef NM, Alving CR. Complement-dependent phagocytosis of liposomes. *Chem Phys Lipids*. 1993;64:239–248.
13. Devine DV, Wong K, Serrano K, Chonn A, Cullis PR. Liposome-complement interactions in rat serum: implications for liposome survival studies. *Biochim Biophys Acta*. 1994;1191:43–51.
14. Ley K, Bullard DC, Arbones ML, Bosse R, Vestweber D, Tedder TF, Beaudet AL. Sequential contribution of L- and P-selectin to leukocyte rolling in vivo. *J Exp Med*. 1995;181:669–675.
15. Pries AR. A versatile video image analysis system for microcirculatory research. *Int J Microcirc Clin Exp*. 1988;7:327–345.
16. Lipowski HH, Zweifach BW. Application of the "two-slit" photometric technique to the measurement of microvascular volumetric flow rates. *Microvasc Res*. 1978;15:93–101.
17. Reneman RS, Woldhuis B, oude Egbrink MGA, Slaaf DW, Tangelder GJ. Concentration and velocity profiles of blood cells in the microcirculation. In: Hwang NHC, Turitto VT, Yen MRT, eds. *Advances in Cardiovascular Engineering.* New York, NY: Plenum Press; 1992:25–40.
18. Jung U, Bullard DC, Tedder TF, Ley K. Velocity differences between L- and P-selectin-dependent neutrophil rolling in venules of mouse cremaster muscle in vivo. *Am J Physiol*. 1996;271:H2740–H2747.
19. Kunkel EJ, Ley K. Distinct phenotype of E-selectin-deficient mice: E-selectin is required for slow leukocyte rolling in-vivo. *Circ Res*. 1996; 79:1196–1204.
20. Jung U, Norman KE, Scharffetter-Kochanek K, Beaudet AL, Ley K. Transit time of leukocytes rolling through venules controls cytokine-induced inflammatory cell recruitment in vivo. *J Clin Invest*. 1998;102: 1526–1533.
21. Bayfield M, Lindner JR, Kaul S, Ismail S, Goodman NC, Spotnitz WD. Deoxygenated blood minimizes adherence of sonicated albumin microbubbles during cardioplegic arrest and after blood reperfusion: experimental and clinical observations with myocardial contrast echocardiography. *J Thorac Cardiovasc Surg*. 1997;113:1100–1108.
22. Czarnwoska E, Karwatowska-Prokopczuk E. Ultrastructural demonstration of endothelial glycocalyx disruption in the reperfused rat heart: involvement of oxygen free-radicals. *Basic Res Cardiol*. 1995;90: 357–364.
23. Patel KD, Nollert MU, McEver RP. P-selectin must extend a sufficient length from the plasma membrane to mediate rolling of neutrophils. *J Cell Biol*. 1995;131:1893–1902.
24. Springer T. Traffic signals on endothelium for lymphocyte recirculation and leukocyte migration. *Annu Rev Physiol*. 1995;57:827–872.
25. Walzog B, Schuppan D, Heimpel C, Hafezi-Moghadam A, Gaehtgens P, Ley K. The leukocyte integrin Mac-1 (CD11b/CD18) contributes to binding of human granulocytes to collagen. *Exp Cell Res* 218;1995: 28–38.
26. Diamond MS, Garcia-Aguilar J, Bickford JK, Corbi AL, Springer TA. The I domain is a major recognition site on the leukocyte integrin Mac-1 (CD11b/CD18) for four distinct adhesion ligands. *J Cell Biol*. 1993;120: 1031–1043.
27. Diamond MS, Springer TA. A subpopulation of Mac-1 (CD11b/CD18) molecules mediates neutrophil adhesion to ICAM-1 and fibrinogen. *J Cell Biol*. 1993;120:545–556.
28. Davis GE, Thomas JS, Madden S. The $\alpha_4\beta_1$ integrin can mediate leukocyte adhesion to casein and denatured protein substrates. *J Leukoc Biol*. 1997;62:318–328.
29. Miller CR, Bondurant B, McLean SD, McGovern KA, O'Brien DF. Liposome-cell interactions in vitro: effect of liposome surface charge on the binding and endocytosis of conventional and sterically stabilized liposomes. *Biochemistry*. 1998;37:12875–12883.
30. Berger M, O'Shea J, Cross AS, Folks TM, Chused TM, Brown EJ, Frank MM. Human neutrophils increase expression of C3bi as well as C3b receptors upon activation. *J Clin Invest*. 1984;74:1566–1571.
31. Chilian WM, Layne SM. Coronary microvascular responses to reductions in perfusion pressure: evidence for persistent arteriolar vasomotor tone during coronary hypoperfusion. *Circ Res*. 1990;66:1227–1238.
32. Ryeom SW, Silverstein RL, Scotto A, Sparrow JR. Binding of anionic phospholipids to retinal pigment epithelium may be mediated by the scavenger receptor CD36. *J Biol Chem*. 1996;271:20536–20539.
33. Skyba DM, Price RJ, Linka AZ, Skalak TC, Kaul S. Direct in vivo visualization of intravascular destruction of microbubbles by ultrasound and its local effects on tissue. *Circulation*. 1998;98:290–293.